Molecular mechanism of action of Pelargonidin-3-O-glucoside, the main anthocyanin responsible for the anti-inflammatory effect of strawberry fruits

Molecular mechanism of Pelargonidin-3-*O*-glucoside, the main anthocyanin responsible for the anti-inflammatory effect of Strawberry fruits

Running title: Anti-inflammatory effect of strawberry fruit and its major anthocyanin

Larissa Jeremias Duarte[a)], Vitor Clasen Chaves[b)], Marcus Vinicius Pereira dos Santos Nascimento[a], Eunice Calvete[c], Mingchuan Li[d], Elisa Ciraolo[d], Alessandra Ghigo[d], Emilio Hirsch[d], Flávio Henrique Reginatto[b], Eduardo M. Dalmarco[a*]

a)These authors contributed equally to this work

[a]Department of Clinical Analysis, Centre of Health Sciences, Federal University of Santa Catarina, Campus Universitário - Trindade, 88040-970, Florianopolis, SC, Brazil.

[b]Department of Pharmaceutical Sciences, Centre of Health Sciences, Federal University of Santa Catarina, Campus Universitário - Trindade, 88040-970, Florianopolis, SC, Brazil.

[c]Graduate Program in Agronomy, College of Agronomy and Veterinary Medicine, University of Passo Fundo, 99052-900, Passo Fundo, RS, Brazil.

[d]Department of Molecular Biotechnology and Health Sciences, Molecular Biotechnology Center, University of Torino, Via Nizza 52,10126, Torino, Italy.

*Corresponding author: Eduardo Monguilhott Dalmarco. [a]Department of Clinical Analysis, Centre of Health Sciences, Federal University of Santa Catarina, Campus Universitário - Trindade, 88040-970, Florianópolis, SC, Brazil. Tel.: +55 48 9115 4470. FAX: +55 48 3721 5072, E-mail: eduardo.dalmarco@ufsc.br or edalmarco@gmail.com (E.M. Dalmarco).

Abstract

Fragaria x *ananassa* Duch., known as strawberry, is consumed worldwide. Studies have shown that strawberry have important biological activities. We therefore evaluated its anti-inflammatory effect of strawberry fruit crude extract and its major anthocyanin Pelargonidin-3-*O*-glucoside (P3G), analyzing its effect on important inflammatory parameters in an *in vivo* model. We have also carried out an *in vitro* study to identify the specific action of P3G in MAPK (mitogen activated protein kinase) and nuclear transcript factor κB pathways. The results demonstrated that strawberry fruit extract and P3G are able to reduce the inflammatory parameters evaluated in the *in vivo* and *in vitro* models. Moreover, we demonstrated that the molecular mechanism involves the arrest of IkB-α activation and reduction in JNK^{MAPK} phosphorylation. These results shown that the consumption of strawberry can be an important functional food to use in the treatment of inflammatory conditions.

Keywords: Inflammation, Raw 264.7, Pleurisy, Strawberry, Pelargonidin-3-*O*-glucoside.

1. Introduction

In mammalian organisms, the inflammatory reaction initially occurs as protective event to rid the organism of harmful stimuli. Normally, at the start of the inflammatory reactions, both pro- and anti-inflammatory mediators are produced and released. An imbalance between these opposing mediators can cause serious tissue damage to the host organism (Reikeras, 2010). This situation occurs in several immune- and age-related chronic inflammatory diseases, such as rheumathoid arthiritis, lupus erythematosus and atherosclerosis (Nathan & Ding, 2010).

The increase in the life expectancy of the world population has led to the appearance of chronic inflammatory diseases that are often refractory to common treatments, requiring effective novel anti-inflammatory drugs. This has led to ongoing study of synthetic and natural anti-inflammatory agents (Hanke et al., 2016; Newman & Cragg, 2016). The search for a healthier lifestyle has also led to the consumption of functional foods, aimed at reducing the use of traditional medicines. It is known that functional foods can reduce the risk of diseases such as cancer, obesity, inflammatory conditions and cardiovascular pathologies, besides having high nutritional value (Kaur & Das, 2011).

Fragaria x *ananassa* Duch., popularly known as strawberry, is known worldwide and consumed *in natura* or in the form of juices, jams or yogurts produced by the food industry (Cerezo et al., 2010). Several studies have shown that strawberry have important

biological activities, such as antioxidant, anti-inflammatory and antihypertensive (Giampieri et al., 2015) activities, which are related to the presence of secondary metabolites, mainly anthocyanins (Smeriglio et al., 2016). Anthocyanins are water-soluble pigments that occur principally as glycosides and are present in several plants and fruits. Although there are seventeen well-known anthocyanins found in nature, only six of them appear to be important in the human diet, due to their biological activity. Strawberries are one of the main sources of anthocyanins, particularly pelargonidin-3-*O*-glucoside (P3G), the major anthocyanin present in strawberry species (Basu et al., 2014; Miguel, 2011).

It is therefore of interest to verify the anti-inflammatory efficacy of *Fragaria* x *anannassa* fruit crude extract and its major anthocyanin P3G as a potential anti-inflammatory agent, analyzing its effect on leukocyte migration, exudation levels, myeloperoxidase (MPO), adenosine deaminase (ADA) activities and nitric oxide (NOx), tumoral necrosis factor (TNF-α) and interleukin 6 (IL-6) levels, using an *in vivo* murine model of pleurisy. In addition, we have carried out an *in vitro* study to identify the specific action of P3G in intracellular inflammatory pathways related to inflammation reactions, such as p38 mitogen-activated protein kinase ($p38^{MAPK}$) and c-Jun N-terminal kinase (JNK^{MAPK}), and nuclear transcript factors κB (NF- κB) and activated protein 1 (AP-1).

2. **Material and Methods**

2.1.***Phytochemical experiments***

2.1.1. *Plant material*

Fruits of *Fragaria* x *ananassa* (Camarosa cultivar) were cultivated at Universidade de Passo Fundo, in Passo Fundo, in the state of Rio Grande do Sul, Brazil. The plants were grown in greenhouse soil and collected in January 2012, at peak maturation. After collection, the fruits were stored at -20°C until extraction and analysis.

2.1.2. *Extraction*

The extracts were prepared according to a method previously described (Carvalho et al., 2012) with minor modifications. Briefly, 1 g of frozen fruits of strawberry were sonicated (Ultrasonic Cleaner 1450, Unique) with 25 mL of acidified (HCl 1%) methanol (pH 1.0) for 75 min. The extracts were filtered, and the solvent evaporated under reduced pressure to dryness, yielding the crude extracts. All these procedures were performed in triplicate.

2.1.3. *Total phenolic content (TP)*

Total phenolic content was evaluated by two spectrophotometric methods: Folin-Ciocalteu (FC) (Singleton, Orthofer & Lamuela-Raventos, 1999) and Fast Blue BB (FBBB) (Medina, 2011). For the FC method, absorbance was measured at 760 nm while

for the FBBB assay, the measurement was performed at 420 nm (Lambda 25 UV/Vis, PerkinElmer®). Samples and standards were analyzed in triplicate and the results expressed as milligrams of gallic acid equivalent per gram of fresh fruit (mg AGE/g FF). Both assays were evaluated using gallic acid as standard solution, ranging from 40 to 150 µg/mL (r^2 = 0.998).

2.1.4. *Total anthocyanin content*

The total anthocyanin content was measured by the differential pH (Lee, Durst & Wrolstad, 2005) and by HPLC.

2.1.5. *pH differential method*

The determination of total monomeric anthocyanins was performed using the pH differential (Lee, Durst & Wrolstad, 2005) at two wavelengths (520 and 700 nm). The molar absorptivity coefficient (Ɛ) for P3G was 25660 L/M/cm in a methanol solution of 1% HCl. The results were expressed as P3G equivalents in mg per 100 g of fresh fruit (mg PGE/100 g FF).

2.1.6. *HPLC assay*

Anthocyanins were also individually identified and quantified by high performance liquid chromatography (HPLC). Analyses were performed on a LC (PerkinElmer® Series 200), equipped with diode array detector (DAD), quaternary pump, degasser and autosampler. Separation was achieved in a C18 column (150 x 4.6 mm id, 5 µm, PerkinElmer®) under constant flow for 1 mL/minute. The elution system used was based on a linear gradient consisting of methanol (A), with an aqueous solution of 3% formic acid (B) as mobile phase. An isocratic elution of 10% A (0-2 minutes) was followed by a linear gradient to 20% A (2-3 minutes), 20 – 41% A (3-19 minutes), then increasing to 70% A (19-30 minutes). The analyses were conducted at 21 ºC (± 2 °C), with injection volume of 20 µL. The chromatograms were monitored at a wavelength of 520 nm, and the spectra were acquired in the 190-700 nm range. Major peaks were characterized by comparison of retention times with the available reference compound P3G, comparison of UV spectra, and co-injection with reference standards.

2.1.7. *Identification of anthocyanins by LC/PDA/MS/MS*

The analysis of anthocyanins was also performed on an Acquity-UPLCTM coupled to a photodiode array detector (PDA) and a high-resolution mass spectrometer (Xevo® G2 QTof model – WATERS®). Anthocyanins were separated using a Polar-RP column SynergiTM - Phenomenex® (4 µm, 150 x 2.0 mm; at 40 ºC), and the injection volume was 5 µL. The mobile phase constitution was an aqueous solution of 2% formic acid (solvent A) and acetonitrile with 1% formic acid (solvent B). The mode of elution

was based on a linear gradient at constant flow (0.4 $mL.min^{-1}$) with a total run time of 34 min, according to the following conditions: 0-10 min, 5-12% B; 10-29 min, 12-18% B; 29-33 min, 18% B; and 33-34 min, 5% B. The detection was carried out at 520 nm, and the spectral scanning range was 350 – 650 nm (PDA). The mass spectrometry detection parameters were: electrospray ionization source (ESI) set on positive ion mode; capillary voltage 1.0 kV; source block temperature 120°C; desolvation temperature 600°C; nebulizer nitrogen flow rate 80 $L.h^{-1}$; desolvation nitrogen gas flow 800 $L.h^{-1}$; and cone voltage 40 V. The software used for the data acquisition and processing was MassLynx v.4.1. The mass spectra were acquired over a mass range from m/z 200 to 1000, with scan time of 0.5 s. MS/MS analysis was performed using argon as collision gas and the collision energy ramp (10 – 30 eV). All analyses were performed in triplicate.

2.2.***In vivo experiments***

2.2.1. *Animals*

In this experimental protocol, we used female Swiss mice (20–25 g), housed under standardized and controlled conditions (20 ± 2 °C, 12 h light/dark periods) with free access to chow and water. The use of female mice in the carrageenan induced pleurisy model was not influenced by the estrous cycle in the inflammatory parameters (Saleh, Calixto & Medeiros, 1996). All experiments were designed to minimize animal suffering and to use the minimum number of animals required to achieve a valid statistical

evaluation. The experiments were performed according to the regulations of the Brazilian College of Animal Experimentation (COBEA) and approved by the Committee for Ethics in Animal Research of the Federal University of Santa Catarina (CEUA - PP00965).

2.2.2. *Experimental design of the murine model of pleurisy*

To verify the possible anti-inflammatory effect of strawberry extract and its major anthocyanin constituent P3G, the mouse model of pleurisy was used. The pleurisy model was performed as previously reported (Dalmarco, Fröde & Medeiros, 2004). Initially, to establish a dose–response curve, animals were randomly divided in different groups (n = 5/group) and were treated with different doses of strawberry fruit crude extract (CE) (100–400 mg/kg), P3G (0.1–10 mg/kg), or dexamethasone (Dex) (0.5 mg/kg) by the oral route (p.o.). Shortly, after 0.5 h, pleurisy was induced by a single injection of 0.1 mL of sterile saline containing λ-carrageenan 1% (w/v) (Cg) administered by the intra-pleural route (i.pl). The animals were euthanized after 4 h with an overdose of ketamine and xylazine administered by the intraperitoneal route (i.p.) and the pleural cavity was exposed and washed with 1.0 mL of sterile phosphate buffered saline (PBS, pH 7.2) (Laborclin, Pinhais, Paraná, Brazil) containing heparin (20 IU/mL). The pleural fluid was used to measure the inflammatory parameters: total and differential leukocyte count and exudate concentration. Next, to determine the best pre-treatment time, the time-course response (0.5-2 h) was performed using two other groups of animals (n=5/group), which

were pre-treated with the lowest effective dose of CE able to significantly reduce the leukocyte count and exudate concentration in the pleural fluid.

In another set of *in vivo* experiments, the previously selected doses and pre-treatment times were used to perform the MPO and ADA activities, NOx, TNF-α and IL-6 levels. For these experiments, the animals were orally treated with CE (400 mg/kg) or P3G (10 mg/kg) followed by induction of pleurisy by Cg 1% (i.pl.). Alongside all the experiments, a group of animals was challenged with 0.1 mL of Cg 1% (i.pl.) only, and was called the negative control group, while another group received 0.1 mL of saline (0.9% NaCl) (i.pl.), and was considered the blank control group.

2.2.3. *Quantification of the leukocyte content and exudate concentration*

To quantify the leukocyte content, pleural fluid samples were submitted to a veterinarian automatic counter (BC-2800 Vet, Mindray, Nanshan, Shenzhen, China). For the differential leukocyte count, cytospin preparations from the exudates were stained with May–Grünwald–Giemsa. The results were expressed as the total number of cells ($\times 10^6$ cells/mL). The exudate concentration was evaluated by measuring the amount of protein in the pleural fluid leakage using the Lowry technique (Lowry et al., 1951). Briefly, the fluid leakage was centrifuged (800 ×g for 10 min, 4 ^{O}C) and Folin & Ciocalteu's phenol reagent (2 N) was added, which bound to the protein. The bound reagent was slowly reduced, changing in color from yellow to blue. Bovine serum

albumin was used as standard (0-40 µg/mL) and the absorbance was read at 630 nm in an ELISA plate reader (Organon Tecknica, Roseland, New Jersey, USA).

2.2.4. *Quantification of myeloperoxidase (MPO) and adenosine-deaminase (ADA) activities*

In-house assays of both MPO and ADA were employed according to the methods developed by Bradley et al. (1982) and Giusti and Galanti (1984), with minor modifications. Using conventional reagents, the concentration of each enzyme was estimated by means of colorimetric measurements (absorbances of 450 and 630 nm, respectively) in an ELISA plate reader (Organon Tecknica, Roseland, New Jersey, USA). Briefly, one unit of MPO is defined as the activity of the enzyme that oxidizes one mol of H_2O_2/min, whereas one unit of ADA is equivalent to the amount of enzyme required to release 1 mmol of ammonia/min. The results were expressed as mU/mL (MPO) and U/L (ADA).

2.2.5. *Measurement of nitric oxide products (NOx)*

Nitric oxide metabolites present in the pleural fluid were quantified using the Griess assay after using vanadium chloride III to reduce nitrate to nitrite, as previously reported (Liz et al., 2011). After centrifugation of pleural fluid samples (800 ×g for 10 min, 4 ^{O}C), the Griess colorimetric measurement was determined at 540 nm using an

ELISA plate reader (Organon Teknika, Roseland, New Jersey, USA). The NO amount was indirectly determined by interpolation from the nitrite standard curve (0–20 μM), and the results were expressed in μM.

2.2.6. *Quantification of tumor necrosis factor alpha (TNF-a) and interleukin-6 (IL-6) levels*

To measure the TNF-α and IL-6 levels, the fluid leakage samples were collected and immediately centrifuged (800 ×g for 10 min, 4 ^{O}C) for cytokine level analyses. The protocols used a commercially available monoclonal TNF-α and IL-6 ELISA Kits (Peprotech, Rocky Hill, New Jersey, USA). The ranges of values detected by these assays were as follows: TNF-α (10-2500 pg/mL) and IL-6 (3-3400 pg/mL). The intra- and interassay coefficients of variation (CV) for TNF-α and IL-6 were as follows: intra CV: TNF-α = 7.8% and IL-6 = 10%; inter CV: TNF-α = 9.6% and IL-6 = 12%, with sensitivity values of TNF-α = 10.0 pg/mL and IL-6 = 3.0 pg/mL. Cytokine levels in the pleural fluid were estimated by interpolation from the standard curve of each cytokine, according to the manufacturer's instructions. The results were expressed in pg/mL.

2.3.***In vitro experiments***

2.3.1. *Cell culture and LPS stimulation*

RAW 264.7 cells were purchased from American Type Cell Culture (ATCC, Rockville, MD) and maintained in Dulbecco's modified Eagle's medium (DMEM) (Gibco, Grand Island, NY, USA) supplemented with 10% fetal bovine serum and 100 U/mL of penicillin, and 100 mg/mL of streptomycin and maintained at 37^{o}C in a humidified CO_2 incubator. Cells were pre-incubated with or without various concentrations (0-128 μM) of P3G or with 7 μM of Dex for 1 hour, then the medium was exchanged with fresh DMEM mixed with lipopolysaccharide (LPS) at a final concentration of 1 μg/mL.

2.3.2. *Citotoxicity*

The cytotoxicity of P3G was assessed by the MTT assay. Briefly, RAW 264.7 cells (5×10^5 cells/well) were treated with different concentrations (1-128 μM) of P3G without LPS treatment. After 24 hours, the medium was removed and the cells were incubated with 0.5 mg/mL MTT solution for 2 hours. The supernatant was then discarded and the formazan blue that formed in the cells was dissolved with dimethyl sulfoxide (DMSO). Optical density was measured at 540 nm with a microplate reader (Infinite M200, Tecan, Männedorf, Switzerland).

2.3.3. *Measurement of NO products*

Nitrite accumulation in the culture supernatants was measured as an indicator of NO production based on the Griess reaction. Unlike the *in vivo* experiments, in these experiments, it was not necessary to reduce nitrate to nitrite with vanadium chloride III. Briefly, 100 µL of cell culture medium was collected 24 h after LPS stimulation, mixed with an equal volume of Griess reagent, and incubated at room temperature for 10 minutes. Absorbance at 540 nm was measured with interpolation from the nitrite standard curve (0–20 µM). Nitrite production was determined, and the results were expressed in µM.

2.3.4. *Quantification of tumor necrosis factor alpha (TNF-a) and interleukin-6 (IL-6) levels*

To determine the TNF-α and IL-6 levels in the culture supernatants, the Raw 264.7 macrophages were pre-treated with different doses of P3G (1-128 µM) for 1 h as previously described, followed by stimulation with LPS at a final concentration of 1µg/mL for 24 h. Next, the supernatant was removed and the levels of pro-inflammatory cytokines TNF-α and IL-6 were determined using a commercially available enzyme-linked immunosorbent assay kit, according to the manufacturer's instructions, as previously described for the *in vivo* experiments.

2.3.5. *Preparation of whole cell, cytosolic and nuclear extracts*

For analyses of the effect of P3G on cell signaling linked to activation of TLR4 receptor, the treatment of cells with P3G or Dex was performed with the IC_{50} dose obtained in the TNF-α experiments. Briefly, after the treatment with P3G (10 µM) or Dex (7 µM) (1 h before), the Raw 264.7 cells were stimulated with LPS (1µg/mL) for 30 min. Next, the medium was removed and the cells were washed twice with ice-cold PBS (pH 7.4), harvested using a cell scraper, and lysed in 1× whole cell lysis buffer (20 mM sucrose, 1 mM ethylenediaminetetraacetic acid, 20 µM Tris-HCl, pH 7.4, 1 mM dithiothreitol, 10 mM KCl, 1.5 mM $MgCl_2$) supplemented with protease/phosphatase inhibitor cocktail→ (Cell Signaling Technology, Danvers, MA, USA). The cell pellets were resuspended in lysis buffer on ice for 1 h, and cell debris was removed by centrifugation. In a parallel experiment to obtain the isolate cytosolic and nuclear proteins, part of whole cell extract obtained above was submitted to separation using a Nuclear and Cytoplasmic Extraction Reagent kit (Pierce Biotechnology Inc., Rockford, IL). The protein concentrations in each sample was determined using the Bio-Rad kit (Bio-Rad Laboratories, Hercules, CA, USA), according to the manufacturer's instructions.

2.3.6. *Western Blot Analysis*

Equal amounts of proteins (whole cell extract: 50 µg/well, cytosolic extract: 25 µg/well, nuclear extract: 25 µg/well) were loaded with Laemmli buffer (Sigma-Aldrich

Co., St. Louis, Missouri, USA) onto a 7.5%, 4-15% or 10% SDS polyacrylamide gel electrophoresis unit and then transferred onto a PVDF membrane (Immobilon-P→ Transfer Membrane, Millipore, Molsheim, France). The membranes were incubated in a blocking buffer (5% w/v BSA in TBST) for 1 h, and then incubated overnight with primary antibody rabbit anti-total p38, phospho-p38, total-JNK, phospho-JNK, total-IKKα/β, phospho-IKKα/β, total-p65, phospho-p65, total-cJun, phospho-cJun, total-lamin B (1:1000) or mouse anti-total-IkBα, phospho-IkBα (1:500) and total-vinculin α (1:1000). The membranes were then washed three times with 0.3 % v/v Tween in TBST buffer (Tris-buffered saline, 0.1% Tween 20), incubated at room temperature for 1 h with anti-mouse or anti-rabbit secondary antibodies conjugated with horseradish peroxidase (HRP) (1:500), washed three times with 0.3 % v/v Tween in TBST buffer, and developed by the chemiluminescent signal enhancing reagent (Luminata Forte→ Western HRP, Millipore, Molsheim, France). Finally, the membranes were exposed and quantified by the Chemidoc Touch® imaging system (Bio-Rad Laboratories, Hercules, CA, USA).

2.4.*Reagents and drugs*

The following chemicals used were obtained from: i) Sigma-Aldrich Co. (St. Louis, Missouri, USA): adenosine, carrageenan (degree IV), Evans blue dye, formalin, hydrogen peroxide, hexadecyltrimethyl ammonium bromide, human neutrophil myeloperoxidase, Laemli buffer, o-dianisidine •2HCl (3,3'dimethoxybenzidine), α-

naphthylethylenediamide •2HCl, phenol, sodium azide, sodium dodecyl sulfate, sodium hypochlorite, sodium nitroprusside, sulfanilamide, and vanadium chloride (III);
ii) Synth (Diadema, São Paulo, Brazil): ethanol; iii) Aché Pharmacological Laboratories S.A (Guarulhos, São Paulo, Brazil): dexamethasone; iv) Vetec (Rio de Janeiro, Rio de Janeiro, Brazil): sodium hydrogen phosphate, zinc sulfate; v) BioTech (São Paulo, São Paulo, Brazil): hydrogen peroxide 30%; vi) Reagen (Rio de Janeiro, Rio de Janeiro, Brazil): sodium hydroxide; vii) Roche (São Paulo, São Paulo, Brazil): heparin; viii) Newprov (Pinhais, Paraná, Brazil): May-Grunwald dye; ix) Laborclin (Pinhais, Paraná, Brazil): Giemsa dye; x) Peprotech (Rocky Hill, New Jersey, USA): Mouse TNF-α and IL-6 ELISA kits; xi) Gibco (Grand Island, New York, USA): Dulbecco's modified Eagle's medium (DMEM), fetal bovine serum (FBS), Penicillin-Streptomycin (10,000 U/mL); xii) American Type Cell Culture (ATCC, Rockville, MD): RAW 264.7 macrophages; xiii) Millipore (Molsheim, France): PVDF membranes, chemiluminescent signal enhancing reagent; xiv) BioRad (Hercules, California, USA): SDS polyacrylamide gel electrophoresis, The primary and secondary antibodies for Western blot analysis were purchased from Cell Signaling Technology, Inc. (Boston, MA, USA) and Santa Cruz Biotechnology (Santa Cruz, CA, USA). The other reagents used were of analytical grade and were obtained from several commercial sources.

2.5.*Data analysis*

The experiments were conducted in triplicate and repeated in three different days. Data were expressed as mean ± SEM. All the variables were tested at normal distribution (Komolgorov-Smirnov) and variance (Bartlett's test). Statistical differences between groups were tested by one-way analysis of variance (ANOVA) followed by the Newman-Keuls post-hoc test. The results were analyzed using GraphPad Prism v5.0 software (GraphPad Software Inc., San Diego, California, USA). Values of $P < 0.05$ were considered significant.

3. **Results**

3.1.***Phytochemical analysis***

The extract of strawberry fruits was analyzed in relation of its total phenolic content (TPC) by Folin-Ciocalteu (Singleton, Orthofer & Lamuela-Raventos, 1999) as well as by the Fast Blue BB (Medina, 2011) assays. The results showed TPC of 2.12 mg/g of fresh fruits (± 4.69%) and 2.03 (± 4.88%) by the FC and FBBB assays, respectively.

The total anthocyanin content (TAC) was measured by the pH differential assay (Lee, Durst & Wrolstad, 2005) and by HPLC. The analysis showed TAC of 24.05 (± 4.29%) mg/100 g of fresh fruits by the pH differential assay and 27.62 (± 3.41%) mg/100 g fresh fruits by HPLC analysis (*Supplemental* file 1). To identify the major anthocyanins present in the strawberry extract, a LC/HRMS analysis was also performed. The MS analysis (*Supplemental* file 2) showed P3G (compound 1) as the major anthocyanin, with over 80% of TAC. Other two anthocyanins were identified as cyanidin-3-*O*-glucoside (compound 2) and pelargonidin-*O*-rutinoside (compound 3) (*Supplemental* file 3). Moreover, the LC/HRMS also showed the presence of another four flavonols: kaempferol-dihexoside, quercetin-glucuronide, kaempferol-rutinoside, and kaempferol-glucuronide in the CE.

3.2.***In vivo Results***

3.2.1. *Effects of Fragaria* x *ananassa CE and P3G on leukocyte migration, neutrophil migration and protein concentrations*

The CE from *Fragaria* x *ananassa*, at doses of 300 and 400 mg/kg, significantly reduced the total leukocyte influx to the pleural cavity compared with the negative control group (Cg) (% inhibition: 300 mg/kg: 34.2 ± 10.8 and 400 mg/kg: 44.6 ± 10.5) ($P < 0.01$) (Table 1). This inhibition was due to the ability of CE to reduce neutrophil migration to the pleural cavity at doses of 300 and 400 mg/kg (% inhibition: 300 mg/kg: 26.7 mg/kg ± 7.6 and 400 mg/kg: 61.03 ± 11.3) ($P < 0.05$) (Table 1). Furthermore, the dose of 400 mg/kg, was able to significantly inhibit the increase of protein levels in the pleural fluid (% de inhibition: 400 mg/kg: 46.05 ± 3.3) ($P < 0.01$) (Table 1).

The main anthocyanin found in *Fragaria* x *ananassa*, P3G at doses of 1.0 and 10 mg/kg, significantly reduced the total leukocyte migration to the pleural fluid (% inhibition 1.0 mg/kg: 40.9 ± 4.5 and 10 mg/kg: 58 ± 3.4) ($P <0.01$) (Table 1), due to inhibition of neutrophil migration (% inhibition 1.0 mg/kg: 34.04 ± 6.1; 10 mg/kg: 66.5 ± 3.7, respectively) ($P < 0.001$) (Table 1). In addition, the protein levels were reduced with the P3G treatment at doses of 0.1, 1.0 and 10 mg/kg (% inhibition 0.1 mg/kg: 15.8 ± 6.9; 1.0 mg/kg: 39.1 ± 3.2 and 10 mg/kg: 52.7 ± 3.4) ($P < 0.05$) (Table 1). The anti-inflammatory drug Dex (0.5 mg/kg) also inhibited these parameters at the tested dose (% of inhibition of leukocyte: 62.5 ± 3.7; neutrophils: 63.3 ± 3.6 and protein levels: 57.3 ± 0.9) ($P < 0.01$) (Table 1).

The lowest doses of *Fragaria* x *ananassa* CE and P3G able to reduce leukocyte influx and protein levels in the pleural fluid were 400 mg/kg and 10 mg/kg, respectively. These doses were therefore chosen for the subsequent set of *in vivo* experiments.

3.2.2. *Effects of Fragaria* x *ananassa CE and P3G on MPO and ADA activities and on NOx levels*

The *Fragaria* x *ananassa* CE, at a dose of 400 mg/kg, significantly reduced the MPO and ADA activities (% inhibition: 27.4 ± 6.4 and 29.72 ± 5.3), respectively ($P < 0.05$) (Table 2). The levels of NOx in the fluid leakage also were inhibited at this same dose (% inhibition: 63.7 ± 0.4) ($P < 0.001$) (Table 2). The P3G at a dose of 10 mg/kg was also able to significantly reduce the MPO and ADA activities (% inhibition: 51.1 ± 2.3 and 34.2 ± 4.9), respectively ($P < 0.001$) (Table 2), and the NOx levels (% inhibition: 37.6 ± 4.9) ($P < 0.001$) (Table 2). The anti-inflammatory drug Dex also reduced these inflammatory parameters (% inhibition of MPO: 47.7 ± 5.3; ADA: 31.0 ± 0.5; NOx: 55.5 ± 3.7) ($P < 0.001$) (Table 2).

3.2.3. *Effects of Fragaria* x *ananassa CE and P3G on TNF-α and IL-6 levels*

The *Fragaria* x *ananassa* CE and the P3G were able to significantly reduce the TNF-α and IL-6 levels compared with the negative control group (Cg), 400 mg/kg CE (% inhibition of TNF-α: 29.8 ± 9.9 and IL-6: 62 ± 9.5) ($P < 0.05$) (Table 2), and 10 mg/kg

P3G (% inhibition of TNF-α: 71.9 ± 3.5 and IL-6: 39.2 ± 6.2) ($P < 0.05$) (Table 2). Dex also was able to significantly reduce the TNF-α levels (% of inhibition: 44.9 ± 6.9) and IL-6 levels (% of inhibition: 48.1 ± 7.4) ($P < 0.05$) (Table 2).

3.3.***In vitro Results***

In these experiments, Dex also was used as an anti-inflammatory reference drug, at a dose of 7 µM, which was chosen in a preliminary experiment performed in our laboratory (Data not shown).

3.3.1. *Cytotoxicity*

Cytotoxicity effect of P3G on Raw 264.7 macrophages was determined using the 3-(4,5-dimethylthiazol-2-yl)-2,5-diphenyltetrazolium bromide (MTT) assay. The viability of cells incubated with different concentrations of P3G (1–128 µM) was not affected at all tested concentrations ($P > 0.05$) (Data not shown). In this context, all subsequent experiments were conducted at non-toxic concentrations of P3G.

3.3.2. *Inhibitory effect of P3G on NOx, TNF-α and IL-6 production in LPS treated RAW 264.7 macrophages*

The secretion of NO in LPS-treated macrophages was significantly inhibited by P3G treatment from doses of 64 and 128 µM (% of inhibition: 23.8 ± 5.7 and 40.3 ± 7.1, respectively) with IC_{50} of 83.2 µM ($P < 0.01$) (Figure 1, *inset*). As expected, the anti-inflammatory drug Dex at 7 µM also inhibited the levels of this pro-inflammatory mediator release from Raw 264.7 macrophages (% inhibition: 67.6 ± 5.5) ($P < 0.01$) (Figure 1, *inset*).

The pro-inflammatory cytokine TNF-α was inhibited by P3G treatment from 2 to 128 µM (% of inhibition: 17.3 ± 2.0 to 91.1 ± 0.6) with the IC_{50} of 10.0 µM ($P < 0.01$) (Figure 1). At the same manner, IL-6 also was inhibited by P3G treatment at doses from 4 to 128 µM (% of inhibition: 16.3 ± 2.0 to 89.9 ± 1.7) and the calculated IC_{50} for this parameter was 6.8 µM ($P < 0.01$) (Figure 1). Both pro-inflammatory mediators secretion were inhibited by the treatment with anti-inflammatory reference drug Dex at 7 µM (% of inhibition: TNF-α: 47.8 ± 3.3 and IL-6: 46.5 ± 1.6) ($P < 0.001$) (Figure 1).

3.3.3. *Inhibitory effect of P3G on phosphorylation of MAPK in LPS treated RAW 264.7 macrophages*

MAPKs play critical roles in the cellular response to LPS stimuli. In addition, MAPKs are also known to be important for the transcriptional activation of NF-kB. To investigate whether the inhibition of the inflammatory response by P3G is mediated through the MAPK pathway, we examined the effect of P3G on the LPS-stimulated phosphorylation of $p38^{MAPK}$ and JNK^{MAPK} on RAW 264.7. The effects of P3G on

phosphorylation of these MAPKs were evaluated, with the dose obtained as IC_{50} for TNF-α performed in previous experiments.

$p38^{MAPK}$ phosphorylation was not attenuated by treatment with P3G in LPS-stimulated RAW 264.7 cells (% inhibition: 8.5 ± 4.2) ($P > 0.05$) (Figure 2A and B). However, the reference anti-inflammatory drug Dex was able to reduce $p38^{MAPK}$ phosphorylation (% inhibition: 25.8 ± 5.4) ($P < 0.05$) (Figure 2A and B).

On the other hand, the phosphorylation of JNK^{MAPK} in Raw 264.7 induced by LPS was significantly inhibited by treatment with P3G (% inhibition: 39.1 ± 8.1) ($P < 0.01$) (Figure 2C and D). The reference drug Dex also inhibited the phosphorylation of JNK^{MAPK} (% inhibition: 54.4 ± 6.0) ($P < 0.001$) (Figure 2C and D).

3.3.4. *Inhibitory effect of P3G on NF-κB pathway in LPS treated RAW 264.7 macrophages*

In the next step, we evaluated the effect of P3G on the NF-kB pathway, the main transcription factor involved in the synthesis of pro-inflammatory mediators after TLR4 activation, and in many cases activated by direct action of MAPKs. In this context, in the first experiments, we decided to observe the effect of P3G on IKKα/β kinase. The IKK kinase complex is the core element of the NF-κB cascade, responsible for the phosphorylation of IkBα, an inhibitory subunit that is present in the cytoplasm interacting with the NF-κB heterodimer (p65/p50). In this context, our results showed that P3G was not able to reduce the phosphorylation of IKK kinases, and subsequently their activation

(% inhibition: 12.8 ± 6.7) ($P > 0.05$) (Figure 3A and B). Likewise, the anti-inflammatory drug Dex did not inhibit the IKKs phosphorylation at the tested dose (% inhibition: 11.5 ± 5.7) ($P > 0.05$) (Figure 3A and B).

Looking forward to the downstream NF-kB pathway, we evaluated the effect of P3G under phosphorylation of the IkB-α subunit. In these experiments, we observed a significant reduction of IkB-α phosphorylation by P3G treatment (% inhibition: 94.1 ± 2.9) ($P < 0.001$) (Figure 3A and C). In a similar manner, Dex also inhibited IkB-α phosphorylation (% inhibition: 27.0 ± 7.4) ($P < 0.05$) (Figures 3A and C).

Finally, we observed the effect of P3G under the next downstream constituent of this cascade, the p65 subunit, which is activated after IkB-α phosphorylation. In these experiments, the treatment of macrophages with P3G before LPS stimulation, significantly reduced p65 phosphorylation when compared with the stimulated control group (% inhibition: 37.2 ± 5.3) ($P < 0.05$) (Figure 3A and D). Dex, a reference anti-inflammatory drug, also inhibited this parameter (% inhibition: 30.2 ± 8.1) ($P < 0.05$) (Figures 3A and D).

3.3.5. *Effect of P3G on LPS-Induced Nuclear Translocation of NF-kB p65 in RAW 264.7 macrophages*

We also investigated whether P3G prevents the translocation of the p65 subunit of NF-kB from the cytosol to the nucleus after its release from IkB-α and phophorylation of the p65 subunit. The stimulated control group, where LPS is administered alone,

showed a decrease in cytosolic p65 content, and an increase in nuclear p65 content ($P < 0.001$) (Figure 4A, B and C).

In these experiments, we observed that pre-treatment of cells with P3G significantly reduced the translocation of the NF-kB p65 subunit from the cytosol to the nucleus. In this context, P3G inhibited translocation of this unit and maintained high levels of p65 in cytosol when compared with the LPS-treated group ($P < 0.001$) (Figure 4A and B). To confirm this point, we also observed the reduction of p65 subunit content in the nucleus after P3G treatment, when compared with the LPS-treated group ($P < 0.001$) (Figure 4A and C). The anti-inflammatory reference drug showed the same pattern of results ($P < 0.001$) (Figure 4A, B and C).

3.3.6. *Effect of P3G on activation of AP-1 transcription factor in LPS-treated RAW 264.7 macrophages*

Activated protein 1 (AP-1) is another conductor transcription factor linked to TLR4 activation. AP-1 is assembled through the dimerization of a characteristic bZIP domain (basic region leucine zipper) in the Fos and Jun subunits. Moreover, AP-1 functions are heavily dependent on the specific Fos and Jun subunits, contributing to AP-1 dimers. Because of this, in our experiments we evaluated the effect of P3G under phosphorylation of subunit c-Jun in the whole cell extract. In this context, our experiments showed that P3G is able to inhibit the phosphorylation of the c-Jun subunit at a significant manner (% inhibition: 39.0 ± 4.8) ($P < 0.001$) (Figure 4D and E), as did Dex, a reference

anti-inflammatory drug, at the tested doses (% inhibition: 52.2 ± 3.7) ($P < 0.001$) (Figure 4D and E).

4. Discussion

It is no surprise that natural products, including anthocyanins, have many biological properties. For this reason, secondary plant metabolites are often reported to be the best candidates for therapeutic drugs, due to their chemical diversity, structural complexity, affordability, and inherent biological activities. Many reports have shown anti-inflammatory action of secondary plant metabolites, both in vitro and in vivo, (Hidalgo et al., 2012; Tall et al., 2004; Zhu et al., 2013). In this study, we investigated the possible anti-inflammatory effect of Fragaria x ananassa Duch. CE, and its major anthocyanin P3G, also known as Callisthephin, on a murine model of pleurisy. To confirm this effect, and to clarify data on the mechanism of action of P3G, we also performed a macrophage cell culture (Raw 264.7) stimulated with LPS.

The phenolic profile of strawberry fruits has previously been reported to contain several bioactive compounds. These include anthocyanins, flavan-3-ols, dihydroflavonols, proanthocyanidins and ellagitannins, as the major secondary metabolites (La Barbera et al., 2017). In our experiments, the results demonstrated higher amounts of phenolic compounds in the CE, since TPC was 2.12 mg/g of fresh fruits (± 4.69%) and 2.03 (± 4.88%) by the FC and FBBB assays, respectively. As expected, the

anthocyanin composition showed P3G as the major anthocyanin. This finding is in agreement with several previous works (Amaro et al., 2013; Arend et al., 2017).

The results presented in our study demonstrated that CE, and the major anthocyanin of strawberry, P3G, are able to reduce the inflammatory parameters evaluated in the murine model of pleurisy and in the cell culture of murine macrophages. In in vivo experiments, the CE from Fragaria x ananassa and P3G showed an important anti-inflammatory profile, inhibiting carrageenan-induced leukocyte influx to the pleural cavity. This inhibition was due to the reduction in neutrophil migration to this cavity. Subsequently, there was a reduction in MPO activity. MPO, which is expressed in primary neutrophil granules, plays a pivotal role in the inflammatory process, and the increase of this enzyme is directly linked to activation of these cells (Arnhold & Flemmig, 2010). These results suggest that CE and P3G not only reduced leukocyte influx to the pleural cavity due to inhibition of neutrophil migration, but also inhibited their activation. Similar results were obtained by Ologundudu and coworkers (2009), who also demonstrated a reduction in leukocyte levels in rabbits intraperitoneally injected with an extract of anthocyanin from Hibiscus sabdariffa, in the 2, 4-dinitrophenylhydrazine-model of hematotoxicity (Ologundudu et al., 2009). Moreover, Hassimotto et al. (2013) demonstrated, in a peritonitis model, that an anthocyanin-enriched fraction extracted from wild mulberry and cyanidin-3-glucoside (the most abundant anthocyanin in the extract), reduced polymorph nuclear influx in the peritoneal exudates, when administered one hour after carrageenan injection (Hassimotto et al., 2013).

The significant reduction of neutrophil migration to the pleural cavity observed in our results can be explained, at least in part, by the ability of CE and P3G to significantly inhibit ADA activity. ADA is an enzyme responsible for adenosine deamination, which reduces the levels of this important anti-inflammatory autacoid. The decrease in ADA activity by CE and P3G therefore results in maintained levels of adenosine that can bind to the A2a and A3 receptors, inducing a significant reduction in neutrophil adhesion to endothelial cells. As a consequence, its migration to the site of inflammation is reduced (Antonioli et al., 2014). These facts are supported by previous experiments performed in our laboratory using the same inflammatory model, which demonstrated that a significant reduction in ADA activity leads to a reduction in neutrophil migration to the pleural cavity (de Souza et al., 2015).

Exudate formation is another signal of inflammatory reaction. This phenomenon is directly linked to the production of nitric oxide after the phlogistic agent has stimulated the innate immune response, inducing iNOS expression (Cuzzocrea et al., 2000). NO, a soluble gas molecule, is responsible for vascular relaxation and consequently, fluid extravasation from the capillaries to the damaged tissue (Tsuchiya et al., 2007). In this context, our experiments showed that CE and P3G were able to reduce the exudate concentration in the pleural cavity in a dose-dependent manner. Reinforcing these results, CE and P3G were able to reduce NO levels in in vitro and in vivo experiments. Our results are corroborated by Wang et al. (2015), who demonstrated an important inhibitory effect of anthocyanins isolated from Ligustrum fruit on NO levels, in mice models of ear edema, abdomen capillary permeability, and cotton granuloma (Wang et al., 2015). Reinforcing

this finding in another study, Vendrame et al. (2014) showed that obese Zucker rats (OZR) submitted to a blueberry diet, another berry source of anthocyanins, have restored aortic vascular function due to down-regulation of iNOS (Vendrame et al., 2014).

The production and release of cytokines to the extracellular environment is the pivotal event in the establishment of the inflammatory web. In the innate immune system, when toll like receptor 4 (TLR4) is activated, triggering a canonical pathway of NF-kB, a series of cytosolic adapter proteins is recruited and becomes an intracellular downstream signal. This, in turn, results in phosphorylation and activation of the IKK complex. IKKβ subsequently phosphorylates the NF-kB (IkB-α) inhibitor, which leads to its proteasomal degradation, thus allowing the nuclear translocation of NF-kB to induce the production of inflammatory cytokines TNF-α and IL-6, among other processes. (Mansell & Jenkins, 2013). Looking at our results, we observed that P3G interferes with the NF-κB pathway by inhibiting IkB-α phosphorylation. However, it was not able to reduce the phosphorylation of IKK kinases. This result suggests that P3G acts by inhibiting proteasomal degradation of IkB-α. Similarly, a study performed by Zhang et al. (2010) also demonstrated that an anthocyanin cyanidin-3-O-β-glucoside inhibited IL-6 and TNF-α expression via direct suppression of IκB-α phosphorylation in LPS-challenged THP-1 cells (Zhang et al., 2010).

Subsequent to the inhibition of IkB-α by P3G, the phosphorylation of p65 NF-kB subunit, and the translocation of this subunit to the nucleus, were reduced. The same pattern of results was obtained by Chen et al. (2006), who also showed inhibition of both the activation and translocation of NF-kB to the nucleus, by treatment with another two

anthocyanins (cyanidin-3-rutinoside and cyanidin-3-glucoside) on highly metastatic A549 human lung carcinoma cells (Chen et al., 2006). Moreover, Lee et al. (2014) demonstrated that LPS-induced NF-κB p65 translocation to the nucleus was markedly attenuated by anthocyanins isolated from blueberry, blackberry and blackcurrant in bone marrow-derived mice macrophages (Lee et al., 2014). Lastly, a study conducted by Kim and coworkers (2006) demonstrated in vivo that anthocyanins isolated from black soybean have protective effects on myocardial infarction and endothelial adhesion molecule expression, an effect attributed to inhibition of NF-κB activation (Kim et al., 2006).

Further specificity and fine-tuning of the degree and duration of TLR4-induced inflammation are achieved by concomitant activation of the mitogen-activated protein kinases (MAPK), more specifically JNKMAPK and p38MAPK (Bode, Ehlting & Häussinger, 2012). Activation of MAPKs directly regulates the activation of some transcription factors, including AP-1. This activation produces a synergic interaction with a canonical NF-kB pathway, resulting in gene expression by simulating the promoter gene of many mediators, such as the cytokines IL-6 and TNF-α (Mansell & Jenkins, 2013). In this context, our experiments showed that P3G has important inhibitory effect under JNKMAPK phosphorylation, and consequently, on c-Jun, the subunit of the AP-1 transcription factor. With regards to the molecular mechanism of this inhibition, we observed that P3G was able to inhibit the phosphorylation of JNKMAPK, but curiously, did not inhibit p38MAPK phosphorylation. Corroborating with these results, Shin and co-workers (2006) also demonstrated that anthocyanins remarkably reduced a number of

phospho-c-Jun N-terminal kinase (p-JNK) cells and suppressed the activation of JNK in the middle cerebral artery occlusion and reperfusion model of cerebral ischemia in rats (Shin, Park & Kim, 2006). Moreover, Hou et al. (2004) showed, in a validated model for screening cancer chemopreventive agents, that anthocyanins suppressed AP-1 transactivation, blocking the phosphorylation of the c-Jun N-terminal kinase (JNK) signaling pathway, although p38MAPK was not inhibited (Hou et al., 2004).

5. Conclusion

In conclusion, we demonstrated that the important anti-inflammatory effect of strawberry is, at least in part, due to the presence of high amounts of P3G. Moreover, the molecular mechanism of this effect involves the arrest of IkB-α activation and reduction in JNK^{MAPK} phosphorylation. These effects lead to a reduction in NF-κB and AP-1 activation of the transcription factors conductors of the inflammatory pathway triggered by the activation of TLR4. These results shown that the human consumption of strawberry can be an important supplemental food in the treatment of inflammatory conditions.

Acknowledgments

The authors are grateful to Fiona Robson for her assistance in proofreading and correcting the English language of this text. This study was supported with grant from Conselho Nacional de Desenvolvimento Científico e Tecnológico (CNPq) (483713/2012-0) and

fellowships from Coordenação de Aperfeiçoamento de Pessoal de Nível Superior (Capes).

Conflict of interests

The authors declares that there is no conflict of interest regarding the publication of this article.

References

Amaro, L. F., Soares, M. T., Pinho, C., Almeida, I. F., Pinho, O., et al. (2013). Processing and storage effects on anthocyanin composition and antioxidant activity of jams produced with Camarosa strawberry. *International Journal of Food Science & Technology*, 48, 2071–2077.

Antonioli, L., Csoka, B., Fornai, M., Colucci, R., Kokai, E., et al. (2014). Adenosine and inflammation: what's new on the horizon? *Drug Discovery Today*, 19, 1051-1068.

Arend, G. D., Adorno, W. T., Rezzadori, K., Di Luccio, M., Chaves, V. C. et al. (2017). Concentration of phenolic compounds from strawberry (*Fragaria X ananassa* Duch) juice by nanofiltration membrane. *Journal of Food Engineering*, 201, 36-41.

Arnhold, J. & Flemmig, J. (2010). Human myeloperoxidase in innate and acquired immunity. *Archives of Biochemistry and Biophysics*, 500, 92-106.

Basu, A., Nguyen, A., Betts, N.M. & Lyons, T.J. (2014). Strawberry as a functional food: an evidence-based review. *Critical Reviews in Food Science and Nutrition*, 54, 790-806.

Bode, J.G., Ehlting, C. & Häussinger, D. (2012). The macrophage response towards LPS and its control through the p38 (MAPK)–STAT3 axis. *Cellular Signalling*, 24, 1185–1194.

Bradley, P.P., Priebat, D.A., Christensen, R.D. & Rothstein, G. (1982). Measurement of cutaneous inflammation: estimation of neutrophil content with an enzyme marker. *Journal of Investigative Dermatology*, 78, 206–209.

Carvalho, A., Blum-Silva, C.H., Calvete, E., Reginatto, F.H. & Simões, C.M.O. (2012). Anti HSV-1 activity of five strawberry cultivars. *Latin American Journal of Pharmacy*, 31, 133-137.

Cerezo, A.B., Cuevas, E., Winterhalter, P., Garcia-Parrilla, M.C. & Troncoso, A.M. (2010). Isolation, identification, and antioxidant activity of anthocyanin compounds in Camarosa strawberry. *Food Chemistry*, 123, 574-582.

Chen, P., Chu, S., Chiou, H., Kuo, W., Chiang, C., et al. (2006). Mulberry anthocyanins, cyanidin 3-rutinoside and cyanidin 3-glucoside, exhibited an inhibitory effect on the migration and invasion of a human lung cancer cell line. *Cancer Letters*, 235, 248–259.

Cuzzocrea, S., Mazzon, E., Calabro, G., Dugo, L. & De Sarro, A. (2000). Inducible Nitric Oxide Synthase—Knockout Mice Exhibit Resistance to Pleurisy and Lung Injury Caused by Carrageenan. *American Journal of Respiratory and Critical Care Medicine*, 162, 1859–1866.

de Souza, R.R., Bretanha, L.C., Dalmarco, E.M., Pizzolatti, M.G. & Fröde, T.S. (2015). Modulatory effect of Senecio brasiliensis (Spreng) Less. in a murine model of inflammation induced by carrageenan into the pleural cavity. *Journal of Ethnopharmacology*, 168, 373-379.

Giampieri, F., Forbes-Hernandez, T., Gasparrini, M., Alvarez-Suarez, J., Afrin, S., et al. (2015). Strawberry as a health promoter: an evidence based review. *Food & Function*, 6, 1386-1398.

Giusti, G. & Galanti, B. (1984). Adenosine deaminase colorimetric method. *Methods of Enzymatic Analysis*, 315–323.

Hanke, T., Merk, D., Steinhilber, D., Geisslinger, G., Schubert-Zsilavecz, M. (2016). Small molecules with anti-inflammatory properties in clinical development. *Pharmacology & Therapeutics*, 157, 163-187.

Hassimotto, N., Moreira, V., Nascimento, N., Souto, P., Teixeira, C., et al. (2013). Inhibition of Carrageenan-Induced Acute Inflammation in Mice by Oral Administration of Anthocyanin Mixture from Wild Mulberry and Cyanidin-3-Glucoside. *BioMed Research International*, 146716.

Hidalgo, M., Martin-Santamaria, S., Recio, I., Sanchez-Moreno, C., De Pascual-Teresa, B., et al. (2012). Potential anti-inflammatory, anti-adhesive, anti/estrogenic, and angiotensin-converting enzyme inhibitory activities of anthocyanins and their gut metabolites. *Genes & Nutrition*, 7, 295–306.

Hou, D., Kai, K., Li, J., Lin, S., Terahara, N., et al. (2004). Anthocyanidins inhibit activator protein 1 activity and cell transformation : structure-activity relationship and molecular mechanisms. *Carcinogenesis*, 25, 29-36.

Kaur, S. & Das, M. (2011). Functional foods: an overview. *Food Science and Biotechnology*, 20, 865-875.

Kim, H., Tsoy, I., Park, J., Chung, J., Shin, S., et al. (2006). Anthocyanins from soybean seed coat inhibit the expression of TNF-α-induced genes associated with ischemia / reperfusion in endothelial cell by NF- κB-dependent pathway and reduce rat myocardial damages incurred by ischemia and reperfusion in vivo. *FEBS Letters*, 580, 1391–1397.

La Barbera, G., Capriotti, A. L., Cavaliere, C., Piovesana, S., Samperi, R., et al. (2017). Comprehensive polyphenol profiling of a strawberry extract (Fragaria × ananassa) by ultra-high-performance liquid chromatography coupled with high-resolution mass spectrometry. *Analytical and Bioanalytical Chemistry,* 409, 2127-2142.

Lee, J., Durst, R.W. & Wrolstad, R.E. (2005). Determination of total monomeric anthocyanin pigment content of fruit juices, beverages, natural colorants, and wines by the pH differential method: Collaborative study. *Journal of AOAC International*, 88, 1269-1278.

Lee, S., Kim, B., Yang, Y., Pham, T., Park, Y., et al. (2014). Berry anthocyanins suppress the expression and secretion of proinflammatory mediators in macrophages by inhibiting nuclear translocation of NF- κB independent of NRF2-mediated mechanism. *The Journal of Nutritional Biochemistry,* 25, 404–411.

Liz, R., Pereira, D.F., Horst, H., Dalmarco, E.M., Dalmarco J.B., et al. (2011). Protected effect of Esenbeckia leiocarpa upon the inflammatory response induced by carrageenan in a murine air pouch model. *International Immunopharmacology*, 11, 1991-1999.

Lowry, O.H., Rosebrough, N.J., Farr, A.L. & Randall., R.J. (1951). Protein measurement with the Folin phenol reagent. *Journal of Biological Chemistry*, 193, 265–275.

Mansell, A. & Jenkins, B.J. (2013). Dangerous liaisons between interleukin-6 cytokine and toll-like receptor families: a potent combination in inflammation and cancer. *Cytokine & Growth Factor Reviews*, 24, 249–256.

Medina, M.B. (2011). Simple and rapid method for the analysis of phenolic compounds in beverages and grains. *Journal of Agricultural and Food Chemistry*, 59, 1565-1571.

Miguel, M.G. (2011). Anthocyanins: antioxidant and/or anti-inflammatory activities. *Journal of Applied Pharmaceutical Science*, 1, 07-15.

Nathan, C. & Ding, A. (2010). Nonresolving Inflammation. *Cell*, 140, 871-882.

Newman, D.J. & Cragg, G.M. (2016). Natural Products as Sources of New Drugs from 1981 to 2014. *Journal of Natural Products*, 79, 629-661.

Ologundudu, A., Ologundudu, A. O., Ololade, I. A. & Obi, F. O. (2009). Effect of Hibiscus sabdariffa anthocyanins on 2,4- dinitrophenylhydrazine-induced hematotoxicity in rabbits. *African Journal of Biochemistry Research*, 3, 140–144.

Reikeras, O. (2010). Immune depression in musculoskeletal trauma. *Inflammation Research*, 59, 409-414.

Saleh, T.S., Calixto, J.B. & Medeiros, Y.S. (1996). Anti-inflammatory effects of theophylline, cromolyn and salbutamol in a murine model of pleurisy. *British Journal of Pharmacology*, 118, 811–819.

Shin, W., Park, S. & Kim, E. (2006). Protective effect of anthocyanins in middle cerebral artery occlusion and reperfusion model of cerebral ischemia in rats. *Life Sciences*, 79, 130–137.

Singleton, V.L., Orthofer, R. & Lamuela-Raventos, R.M. (1999). Analysis of total phenols and other oxidation substrates and antioxidants by means of Folin-Ciocalteu reagent. *Methods in Enzymology*, 299, 152-178.

Smeriglio, A., Barreca, D., Bellocco, E. & Trombetta, D. (2016). Chemistry, Pharmacology and Health Benefits of Anthocyanins. *Phytotherapy Research*, 30, 1265-1286.

Tall, J.M., Seeram, N.P., Zhao, C., Nair, M.G., Meyer, R.A., et al. (2004). Tart cherry anthocyanins suppress inflammation-induced pain behavior in rat. *Behavioural Brain Research*, 153, 181–188.

Tsuchiya, K., Sakai, H., Suzuki, N., Iwashima, F., Yoshimoto, T., et al. (2007). Chronic blockade of nitric oxide synthesis reduces adiposity and improves insulin resistance in high fat-induced obese mice. *Endocrinology*, 148, 4548–4556.

Vendrame, S., Kristo, A.S., Schuschke, D.A. & Klimis-Zacas, D. (2014). Wild blueberry consumption affects aortic vascular function in the obese Zucker rat. *Applied Physiology, Nutrition, and Metabolism*, 39, 255–261.

Wang, J., Wang, J.A., Jiang, Y.X., Zhou, P.P. & Wang, H.H. (2015). The mechanism of anthocyanin to anti-inflammatory and analgesic from Ligustrum fruit. *Chinese Journal of Applied Physiology*, 31, 431-436.

Zhang, Y., Lian, F., Zhu, Y., Xia, M., Wang, Q., et al. (2010). Cyanidin-3-O-β-glucoside inhibits LPS-induced expression of inflammatory mediators through decreasing IκBα phosphorylation in THP-1 cells. *Inflammation Research*, 59, 723–730.

Zhu, Y., Ling, W., Guo, H., Song, F., Ye, Q., et al. (2013). Anti-inflammatory effect of purified dietary anthocyanin in adults with hypercholesterolemia: A randomized controlled trial. *Nutrition, Metabolism & Cardiovascular Diseases*, 23, 843–849.

Figure Captions

***Supplemental* file 1.** Chromatogram of *Fragaria* x *ananassa* Duch.

***Supplemental* file 2.** MS and MSMS spectra of pelargonidin-3-*O*-glucoside

Figure 1. Effects of pelargonidin-3-*O*-glucoside on TNF-α and IL-6 levels in LPS treated Raw 264.7 macrophages. *Inset,* Effect of pelargonidin-3-*O*-glucoside on NOx levels. DMSO: cells treated with only sterile dimethylsulfoxide; LPS: cells treated with only lipopolysaccharide (1µg/mL); Dex: animals pre-treated with dexamethasone (7 µM) before LPS administration; P3G: cells pre-treated with pelargonidin-3-*O*-glucoside (1-128 µM) before LPS administration; Results were expressed as mean ± SEM; n = 4; ** $P < 0.01$ and *** $P < 0.001$.

Figure 2. Effects of pelargonidin-3-*O*-glucoside on phosphorylation of $p38^{MAPK}$ (A and B) and on phosphorylation of JNK^{MAPK} (C and D) in LPS treated Raw 264.7 macrophages. (A) Western blot representative image of p38 phosphorylation experiments. (B) Graphical representation of p38 phosphorylation experiments. (C) Western blot representative image of JNK phosphorylation experiments. (D) Graphical representation of JNK phosphorylation experiments DMSO: cells treated with only sterile dimethylsulfoxide; LPS: cells treated with only lipopolysaccharide (1µg/mL); Dex: animals pre-treated with dexamethasone (7 µM) before LPS administration; P3G: cells pre-treated with pelargonidin-3-*O*-glucoside (10 µM) before LPS administration; Results were expressed as mean ± SEM; n = 4; * $P < 0.05$, ** $P < 0.01$ and *** $P < 0.001$.

Figure 3. Effects of pelargonidin-3-*O*-glucoside on NF-kB pathway in LPS treated Raw 264.7 macrophages. (A) Western blot representative image of NF-kB pathway phosphorylation experiments; (B) Graphical representation of IKKα/β phosphorylation experiments; (C) Graphical representation of Ikβ-α phosphorylation experiments; (D) Graphical representation of p65 phosphorylation experiments. DMSO: cells treated with only sterile dimethylsulfoxide; LPS: cells treated with only lipopolysaccharide (1µg/mL); Dex: animals pre-treated with dexamethasone (7 µM) before LPS administration; P3G: cells pre-treated with pelargonidin-3-*O*-glucoside (10 µM) before LPS administration; Results were expressed as mean ± SEM; n = 4; * $P < 0.05$ and *** $P < 0.001$.

Figure 4. Effects of pelargonidin-3-*O*-glucoside on NF-kB p65 nuclear translocation (A, B and C) and on AP-1 nuclear transcription factor (D and E) in LPS treated Raw 264.7 macrophages. (A) Western blot representative image of NF-kB p65 cytosolic and nuclear fractions experiments; (B) Graphical representation of NF-kB p65 cytosolic fraction experiments; (C) Graphical representation of NF-kB p65 nuclear fraction experiments. (D) Western blot representative image of c-Jun experiments; (E) Graphical representation of c-Jun experiments. DMSO: cells treated with only sterile dimethylsulfoxide; LPS: cells treated with only lipopolysaccharide (1µg/mL); Dex: animals pre-treated with dexamethasone (7 µM) before LPS administration; P3G: cells pre-treated with pelargonidin-3-*O*-glucoside (10 µM) before LPS administration; Results were expressed as mean ± SEM; n = 4; *** $P < 0.001$.

Highlights

* Strawberry fruit has an important anti-inflammatory effect.

* Pelargonidin-3-O-glucoside is the main anthocyanin responsible for the anti-inflammatory effect.

* The mechanism of this effect involves the NF-κB and MAPK pathways.

* Strawberry fruit can be an important supplemental food in the treatment of inflammatory conditions.

Graphical abstract

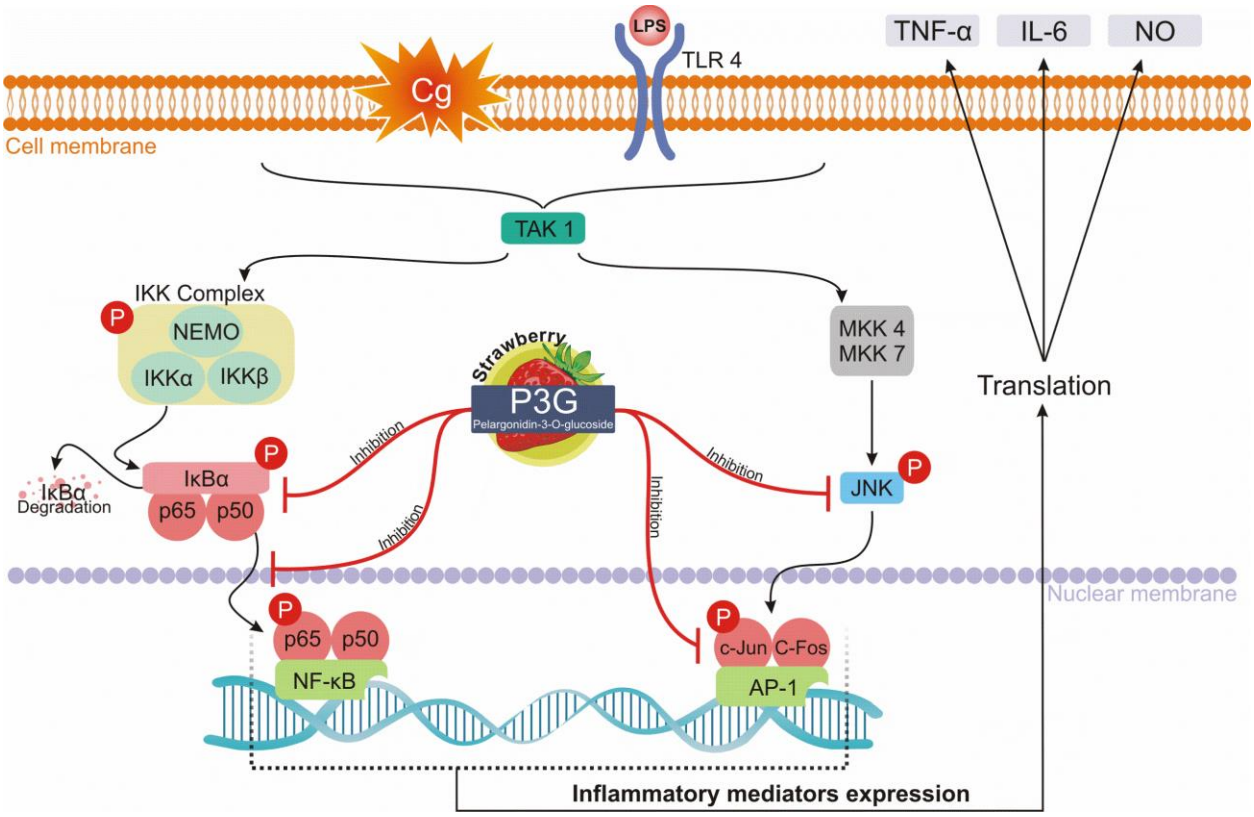

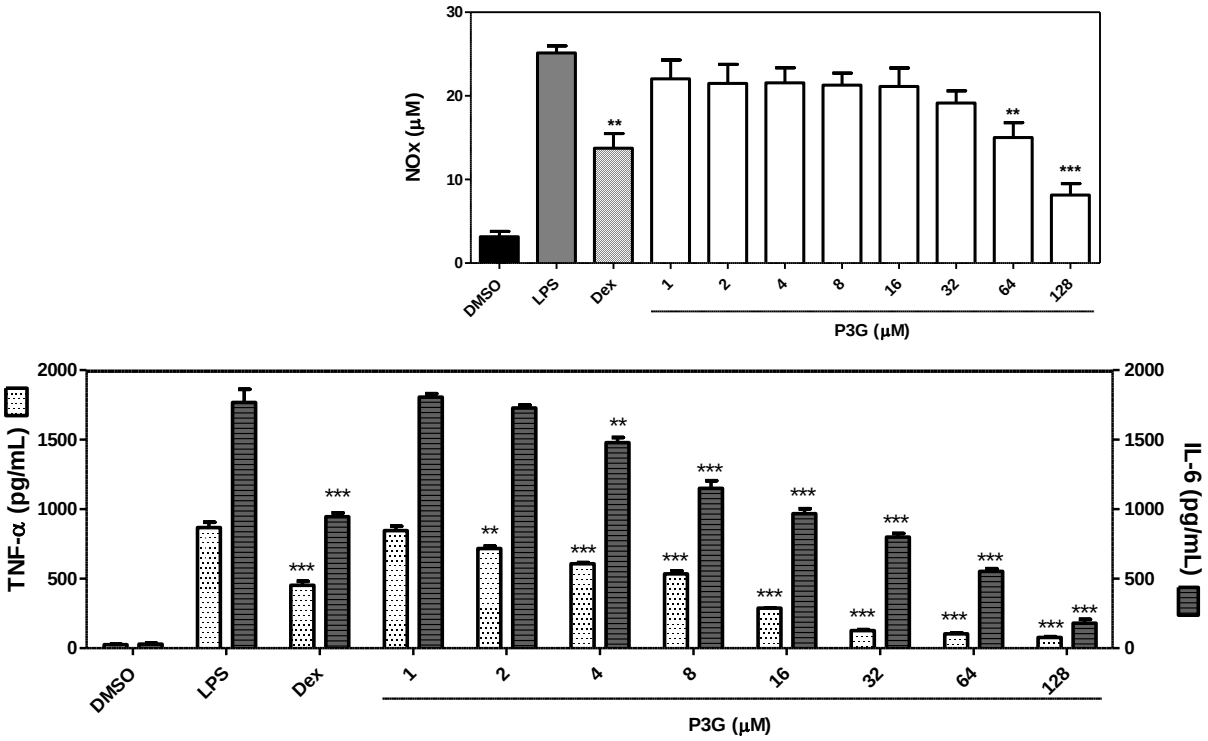
NOx (μM)
30
20
10
0
**
**
***
DMSO
LPS
Dex
1
2
4
8
16
32
64
128
P3G (μM)
TNF-α (pg/mL)
IL-6 (pg/mL)
2000
1500
1000
500
0
**
***
DMSO
LPS
Dex
1
2
4
8
16
32
64
128
P3G (μM)

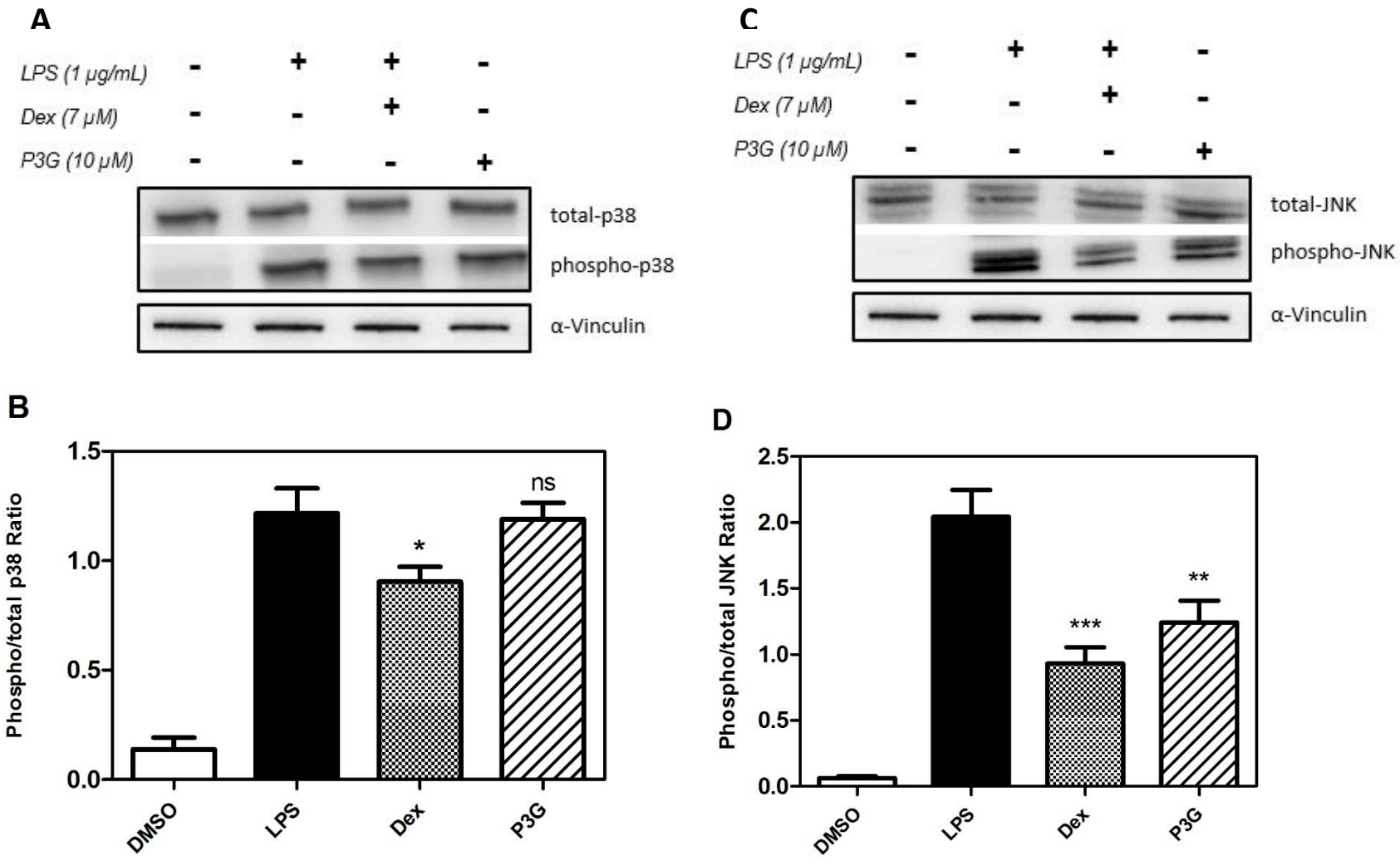
A
LPS (1 μg/mL)
Dex (7 μM)
P3G (10 μM)
total-p38
phospho-p38
α-Vinculin
C
LPS (1 μg/mL)
Dex (7 μM)
P3G (10 μM)
total-JNK
phospho-JNK
α-Vinculin
B
Phospho/total p38 Ratio
1.5
1.0
0.5
0.0
*
ns
DMSO
LPS
Dex
P3G
D
Phospho/total JNK Ratio
2.5
2.0
1.5
1.0
0.5
0.0
***
**
DMSO
LPS
Dex
P3G

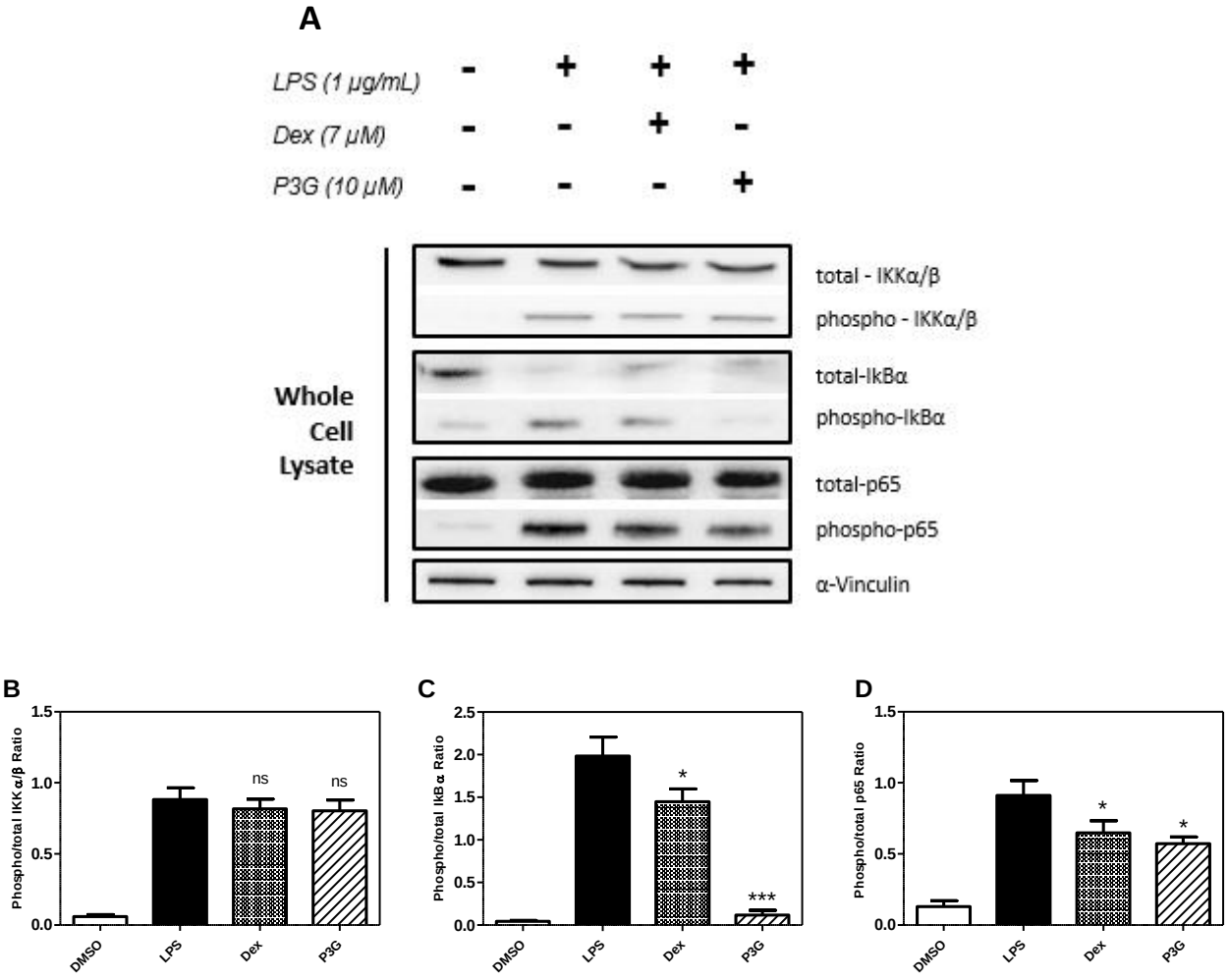
A
LPS (1 µg/mL)
Dex (7 µM)
P3G (10 µM)
- + + +
- - + -
- - - +
Whole Cell Lysate
total - IKKα/β
phospho - IKKα/β
total-IkBα
phospho-IkBα
total-p65
phospho-p65
α-Vinculin
B
Phospho/total IKK α/β Ratio
ns
ns
DMSO
LPS
Dex
P3G
C
Phospho/total IkBα Ratio
*
***
D
Phospho/total p65 Ratio
*
*

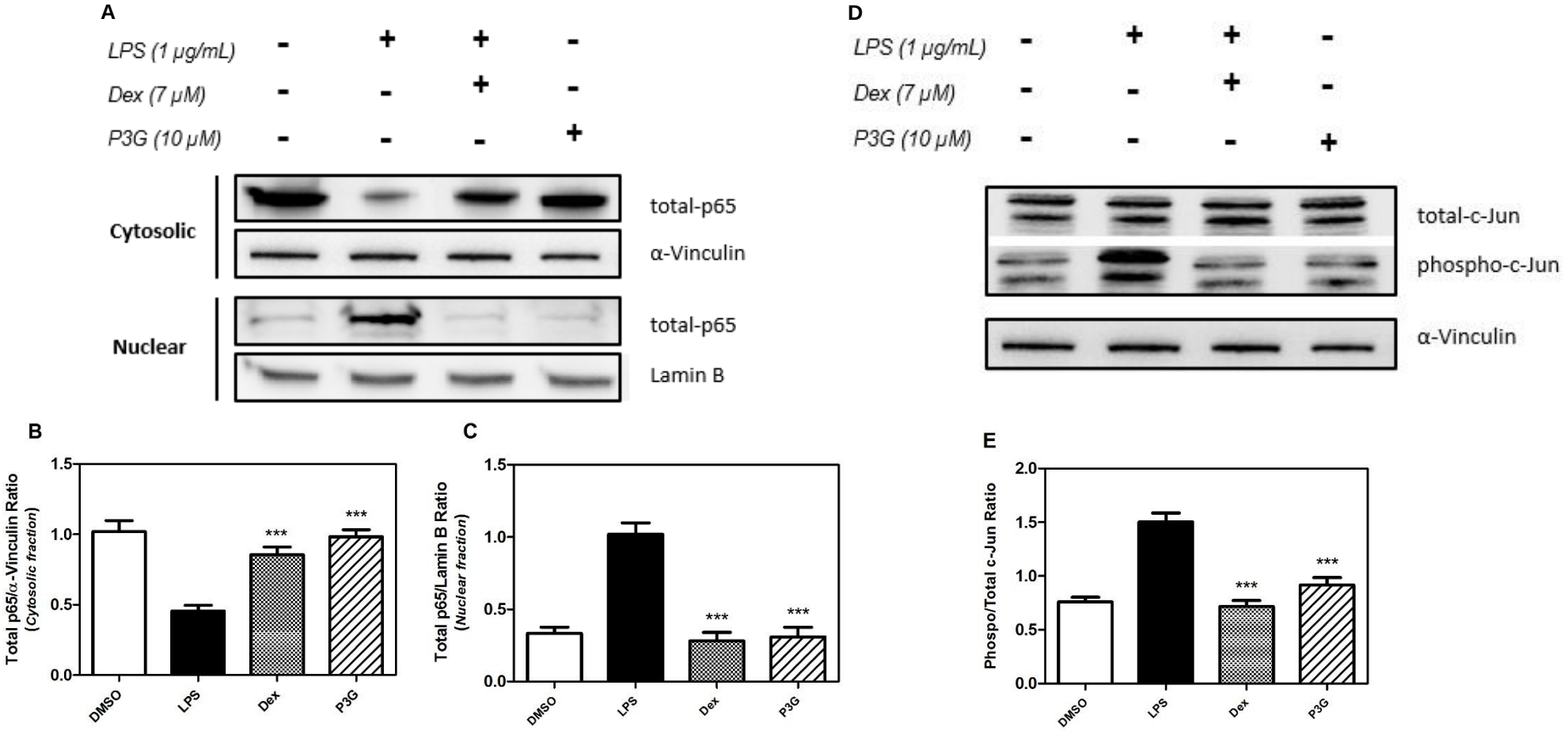
A
LPS (1 μg/mL) - + + -
Dex (7 μM) - - + -
P3G (10 μM) - - - +
Cytosolic
total-p65
α-Vinculin
Nuclear
total-p65
Lamin B
D
LPS (1 μg/mL) - + + -
Dex (7 μM) - - + -
P3G (10 μM) - - - +
total-c-Jun
phospho-c-Jun
α-Vinculin
B
Total p65/α-Vinculin Ratio (Cytosolic fraction)
1.5
1.0
0.5
0.0
***
***
DMSO
LPS
Dex
P3G
C
Total p65/Lamin B Ratio (Nuclear fraction)
1.5
1.0
0.5
0.0
***
***
DMSO
LPS
Dex
P3G
E
Phospo/Total c-Jun Ratio
2.0
1.5
1.0
0.5
0.0
***
***
DMSO
LPS
Dex
P3G

Table 1. Effects of *Fragaria* x *ananassa* crude extract and P3G upon total leukocytes migration, neutrophils migration and proteins concentrations, in the mouse model of pleurisy induced by carrageenan.

Groups/doses (mg/kg)	Leukocytes (10^6)	Neutrophils (10^6)	Proteins (µg/mL)
S	1.7 ± 0.07	0.2 ± 0.03	26.6 ± 1.7
Cg	6.0 ± 0.3	4.7 ± 0.2	209 ± 17.3
Dex (0.5)	2.6 ± 0.2**	1.6 ± 0.2***	89.2 ± 2.0***
CE (100)	5.4 ± 0.3	4.1 ± 0.3	202.3 ± 11.7
CE (200)	4.6 ± 0.5	3.7 ± 0.4	196.4 ± 20.4
CE (300)	3.9 ± 0.6**	3.4 ± 0.3*	186.2 ± 23.3
CE (400)	3.3 ± 0.6**	1.8 ± 0.5***	112.7 ± 6.9**
P3G (0.1)	6.3 ± 1.1	4.2 ± 0.2	175.9 ± 14.4*
P3G (1.0)	4.1 ± 0.3**	3 ± 0.3***	127.1 ± 6.7***
P3G (10)	2.9 ± 0.2***	1.6 ± 0.2***	98.8 ± 7.2***

Crude extract (CE) and Callistephin (P3G) were administered by oral route (p.o.) 0.5 h before carrageenan-induced inflammation. The negative control groups were treated only with sterile saline (0.95% NaCl) by the intrapleural route. The positive control groups were treated only with carrageenan (1%) by the intrapleural route. Dexamethasone (Dex) was used as reference anti-inflammatory drug and was administered by oral route (p.o.). The data are reported as the mean ± SEM, n = 5 animals. *$P < 0.05$, **$P < 0.01$, ***$P<0.001$.

Table 2. Effects of *Fragaria* x *ananassa* crude extract and P3G upon myeloperoxidase (MPO), adenosine deaminase (ADA) activities, nitric oxide metabolites (NOx), TNF-α and IL-6 levels in the mouse model of pleurisy induced by carrageenan.

Groups/doses (mg/kg)	MPO (mU/L)	ADA (U/L)	NOx (µM)	TNF-α (pg/mL)	IL-6 (pg/mL)
S	66.4 ± 3.2	2.4 ± 0.02	61.9 ± 1.5	8.9 ± 3.5	7.0 ± 4.0
Cg	169.1 ± 4.9	7.6 ± 0.5	183.0 ± 20.7	316.1 ± 25.6	879 ± 171
Dex (0.5)	84.9 ± 9***	5.2 ± 0.04***	81.4 ± 6.8***	174.4 ± 22.05**	456.5 ± 65.1*
CE (400)	132.0 ± 19.4*	5.3 ± 0.4***	66.4 ± 0.7***	233.9 ± 43.5*	334 ± 84.1**
P3G (10)	82.6 ± 3.9***	5.0 ± 0.4***	114.1 ± 8.9***	88.9 ± 11.1***	534 ± 54.5*

Crude extract (CE) and Callistephin (P3G) were administered by oral route (p.o.) 0.5 h before carrageenan-induced inflammation. The negative control group (S) was treated only with sterile saline (0.95% NaCl) by the intrapleural route. The positive control group (Cg) was treated only with carrageenan (1%) by the intrapleural route. Dexamethasone (Dex) was used as reference anti-inflammatory drug and was administered by oral route (p.o.). CE: animals pre-treated with crude extract (400 mg/kg, p.o.) before Cg administration; P3G: animals pre-treated with Callistephin (10 mg/kg, p.o.) before Cg administration; n = 5 animals; *$P < 0.05$, **$P < 0.01$, *** $P<0.001$.

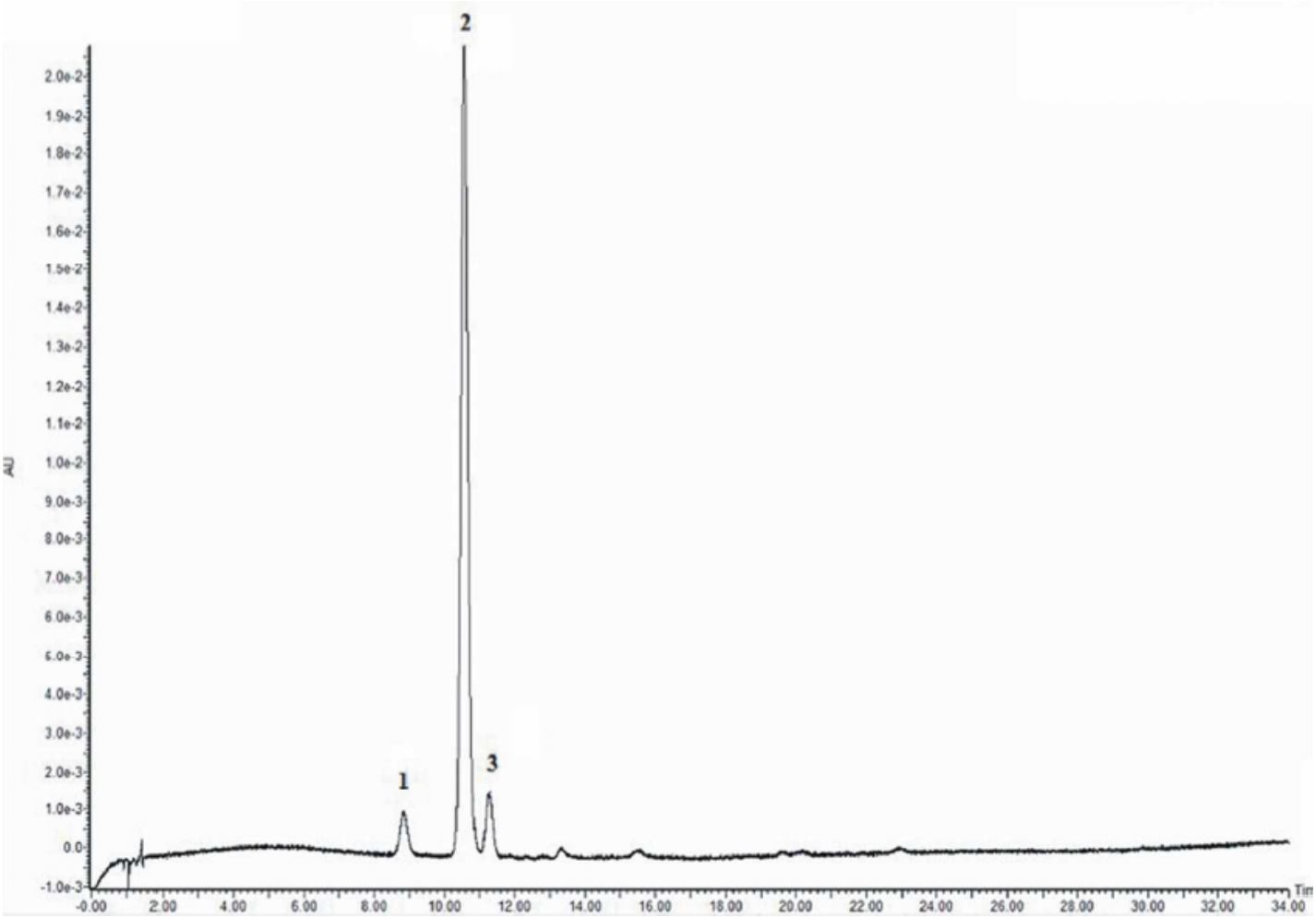
2
1
3
AU
2.0e-2
1.9e-2
1.8e-2
1.7e-2
1.6e-2
1.5e-2
1.4e-2
1.3e-2
1.2e-2
1.1e-2
1.0e-2
9.0e-3
8.0e-3
7.0e-3
6.0e-3
5.0e-3
4.0e-3
3.0e-3
2.0e-3
1.0e-3
0.0
-1.0e-3
-0.00
2.00
4.00
6.00
8.00
10.00
12.00
14.00
16.00
18.00
20.00
22.00
24.00
26.00
28.00
30.00
32.00
34.00

***Supplemental* file 2**

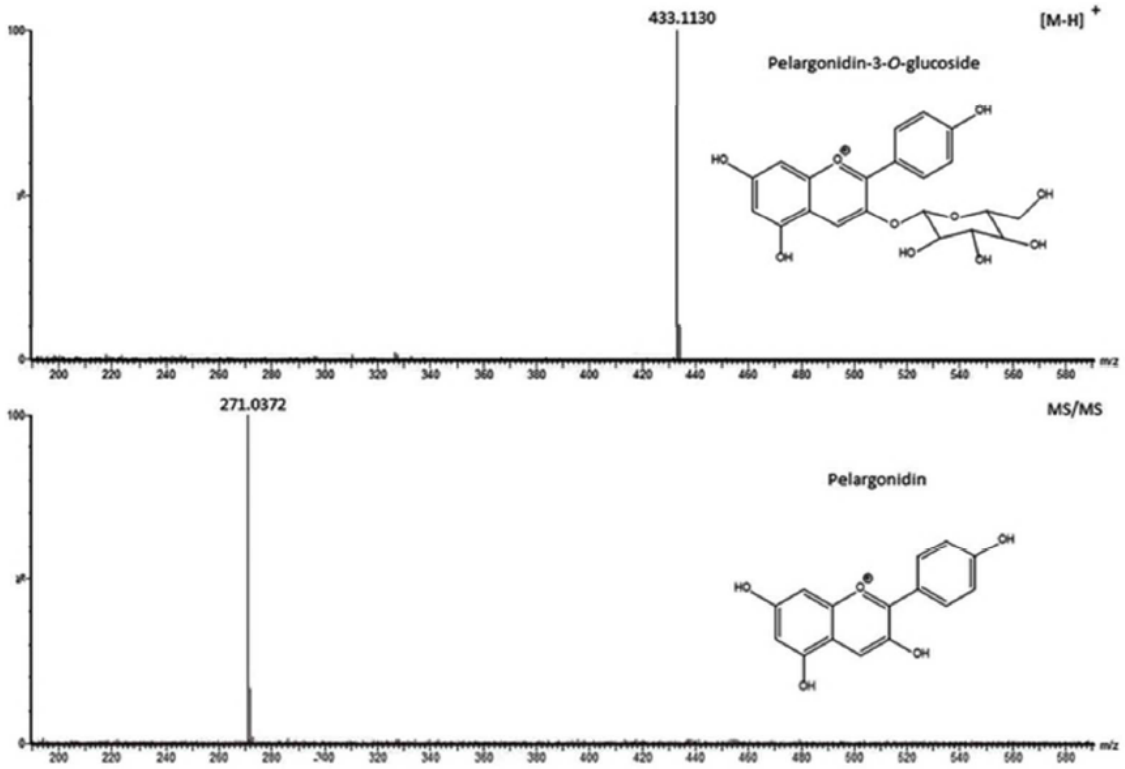

***Supplemental* file 3** – Identification of anthocyanins in *Fragaria* x *ananassa* extract.

Retention time (min)	λ_{max} (nm)	Molecular formula	$[M-H]^+$ *m/z*	Error (ppm)	Main fragments *m/z*	TAC (%)	Identification
8.49	516	$C_{21}H_{21}O_{11}$	449.1065	-4.2	287	5.65	Cyanidin-3-*O*-glucoside
10.29	500	$C_{21}H_{21}O_{10}$	433.1130	1.2	271	80.18	Pelargonidin-3-*O*-glucoside
11.09	500	$C_{27}H_{31}O_{14}$	579.1721	1.2	433; 271	14.17	Pelargonidin-*O*-rutinoside

TAC - total anthocyanin content